Computational Engineering and Physical Modeling 1-1 (2018) 38-57

Contents lists available at **CEPM**

Computational Engineering and Physical Modeling

Journal homepage: www.jcepm.com

Seismic Fragility Assessment of Local and Global Failures in Low-rise Non-ductile Existing RC Buildings: Empirical Shear-Axial Modelling vs. ASCE/SEI 41 Approach

M.R. Azadi Kakavand[1]*, M. Khanmohammadi[2]

1. Unit of Strength of Materials and Structural Analysis, Department of basic sciences in engineering sciences, University of Innsbruck, Innsbruck, Austria
2. Faculty of Civil Engineering, University of Tehran, Tehran, Iran

Corresponding author: *mohammad.azadi-kakavand@uibk.ac.at*

https://doi.org/10.22115/CEPM.2018.114549.1008

ARTICLE INFO

Article history:
Received: 12 January 2018
Revised: 17 March 2018
Accepted: 19 March 2018

Keywords:
Shear and axial failures;
Local and global collapse;
Non-ductile reinforced concrete buildings;
Fragility curves.

ABSTRACT

The brittle behavior of older non-ductile reinforced concrete buildings such as shear-axial failure in columns can cause lateral instability or gravity collapse. Hence, the attempt is to assess the collapse potential through fragility curves. Current research focuses on fragility assessment of these buildings emphasizing on shear-axial failure using two well-established methods; empirical limit state material versus ASCE/SEI 41-13 recommendations. To this aim, two 2D reinforced concrete models (3 and 5-story) according to typical detail of existing buildings in Iran were modeled using two aforementioned modeling approaches and analyzed under monotonic analysis and incremental dynamic analysis (IDA). In the following, seismic fragility assessment were carried out by means of obtained results from IDA. The results of fragility curves showed that collapse capacity of buildings modeled by ASCE/SEI 41-13 are more than empirical method and fewer cases can pass the level of safety probability of failure suggested by ASCE/SEI-41.

1. Introduction

A significant portion of constructed buildings during 20th century particularly those in under developed countries do not satisfy seismic provisions proposed by new seismic regulations. In

How to cite this article: Azadi Kakavand MR, Khanmohammadi M. Seismic Fragility Assessment of Local and Global Failures in Low-rise Non-ductile Existing RC Buildings: Empirical Shear-Axial Modelling vs. ASCE/SEI 41 Approach. Comput Eng Phys Model 2018;1(1):38–57. https://doi.org/10.22115/CEPM.2018.114549.1008

this regard, post inspections of past earthquakes revealed that such vulnerable buildings might experience severe damages due to lack of adequate ductility and shear strength. Although, modern buildings considerably secured life safeties under excitation of previous earthquakes it was shown that they probably would not satisfy higher performance objectives coming from higher life standards such as collapse prevention or global instability which may induce beyond acceptable economical impacts [1]. Therefore, many research activities have been conducted to shift conventional approaches to the new generation of seismic design so-called Performance-Based Seismic Design (PBSD). With developing the PBSD approaches in both assessment or design of old and new buildings, the attention on seismic collapse capacity of buildings, particularly non-ductile, has been emerged as a main concern on the survivability of human life. In the following, it was particularly noticed that defining reliable and accurate limit states or performance criteria play a key role in the application of PBSD. In this regard, several inconsistencies were shown in common proposed threshold values such as rotations, strains, ductility and inter-story drift. For instance, equivalent local (e.g., rotations or strains) and global (e.g., inter-story drift ratio) criteria for a moment-resisting RC frame can result in different safety levels [2]. Hence, many experimental and analytical types of research have been conducted by different researchers to explore one of the most widely observed failures in existing RC components, i.e., the shear -axial behavior interaction including both strength and deformation capacities. In addition, experimental and numerical studies of steel-concrete composite structures are being conducted to improve the shear capacity and ductility of buildings during the earthquake [3–7] However, the main focus is reinforced concrete structures. The past experimental tests have aimed to discover the effects of shear failure on axial failure regarding involved influenced parameters [7–19]. Almost all the conducted tests have been carried out on single columns as a whole or non-ductile column as a part of the frame. Additionally, the results of experimental tests were compared with those obtained from analytical models adopted from empirical proposed equations [8] for flexure-shear-axial interaction (Eq. 1 and 2) or numerical models consistent with compression field theory [20–26]. It is worthwhile to note that largely occurred nonlinearity doubted applicability of common nonlinear analyses such as pushover for these aims. In this regard, it was noticed that they might lead to acceptable outcomes regarding mean values, but a significant drift under-estimation possibility and misleading damage location should be expected [27]. Nevertheless, it was concluded that the proposed model by Elwood and corresponding developed Limit State material [28] in OpenSees [29] seems to be one of the most practical approaches. This Limit State material has been based on Equation 1 and 2 in which drift ratio at shear, and axial failures are addressed, respectively.

$$\left(\frac{\Delta_s}{L}\right) = \frac{3}{100} + 4\rho'' - \frac{1}{40}\frac{v}{\sqrt{f'_c}} - \frac{1}{40}\frac{P}{A_g.f'_c} \geq \frac{1}{100} \qquad (MPa) \tag{1}$$

$$\left(\frac{\Delta}{L}\right)_{axial} = \frac{4}{100}\frac{1 + (tan\theta)^2}{tan\theta + P(\frac{s}{A_{st}F_{st}d_c tan\theta})} \quad (MPa)\ or\ (psi) \tag{2}$$

In Eq. 1 and 2, ρ'' is the transverse reinforcement ratio, v is nominal shear stress, f'_c is the compressive strength of concrete, P is the axial load on column and A_g is the gross cross-sectional area, Θ is the crack angel from horizontal, s is the spacing of the transverse

reinforcement, A_{st} is the area of the transverse reinforcement, F_{st} is the yield strength of the transverse reinforcement and *dc* is the effective depth of column section. However, the aforementioned equations are recently modified to increase its accuracy in prediction of the onset of shear and axial failure in RC columns. Elwood et al. proposed ASCE/SEI 41 update and introduced new modeling parameters for shear- axial behavior in non-linear columns using the results of past researches [30]. Eventually, their proposed simple global modeling parameters were included in last published ASCE-41 in 2013 [31].They implicitly considered shear-axial failures into global moment-rotation response of deficient columns. In the literature, a few analytical paper has been published on seismic fragility assessment or probabilistic assessment of non-ductile R.C. buildings [32–34]. A research was presented by [35] as a part of ATC78 project to assess a structure with 6 story and 5 bays perimeter moment- resisting frame for collapse risk. They found that the ratio of column plastic shear to shear capacity and ratio of columns to beams moment capacities are the important collapse indicators in non-ductile frames. Baradaran Shoraka et al., conducted an analytical approach to find seismic loss estimation of such building [36]. To this end, a seven-story eight-bay nonductile building located in Los Angeles was investigated. They found that the first failure overestimates the financial loss due to ignoring redistribution of loads. Although the behavior of columns susceptible to suffer shear-axial failure has been well addressed in the literature, however less analytical assessment on existing non-ductile R.C buildings, as a whole, has been carried out. Since the geometry and mechanical properties, structural system, and practice of construction can affect the resulted responses, generally the results of past few researches on such buildings cannot be assigned to elsewhere. The existing old non-ductile RC buildings in Iran are different with others from point of geometry (normally 3-5 story), material strength (very poor to fair), rebar type (the most of them are plain instead of deformed bar), arrange of both longitudinal and particularly transverse ties(one circumference hoop without interior ties and seismic hooks, spaced each 0.5H-H) [37]. In the current research, the effect of axial load ratio (*P/Ag.f'c*), the ratio of plastic shear to shear capacity (*Vp/Vn*), on collapse capacity of two representative non-ductile RC buildings are investigated, where, *Vp* is the plastic shear demand on the column (shear demand at flexural strength of the plastic hinges), and *Vn* is the shear strength of the column [8]. To this end, using calibrated model and two different approaches, the seismic fragility of structures are assessed, and finally, the effects of mentioned parameters are investigated.

2. The validation of numerical modeling technique

2.1. The description of the analyzed frame

The aim of this study focuses on the seismic fragility assessment of local and global failures in low-rise non-ductile existing RC buildings by means of two techniques, empirical modeling, and ASCE/SEI concrete provisions. To validate the modeling method of columns for simulation of shear-axial failures, an experimental test is selected [38]. The tested model is a frame with two stories and two bays. The dimensions and general view of the tested specimen are shown in Figure 1. The ratios of *Vp/Vn* and *P/Ag.f'c* were 0.84 and 0.2 respectively. The Young's modulus and the Poisson's ratio for concrete were set to 18200 MPa and 0.2, respectively. For reinforcing steel, The Young's modulus and the Poisson's ratio were set to 138 GPa and 0.3, respectively.

The compressive strength of concrete was 28 MPa, and the yield strengths of the longitudinal and transverse bars in the columns were 444 MPa and 417 MPa respectively [41].

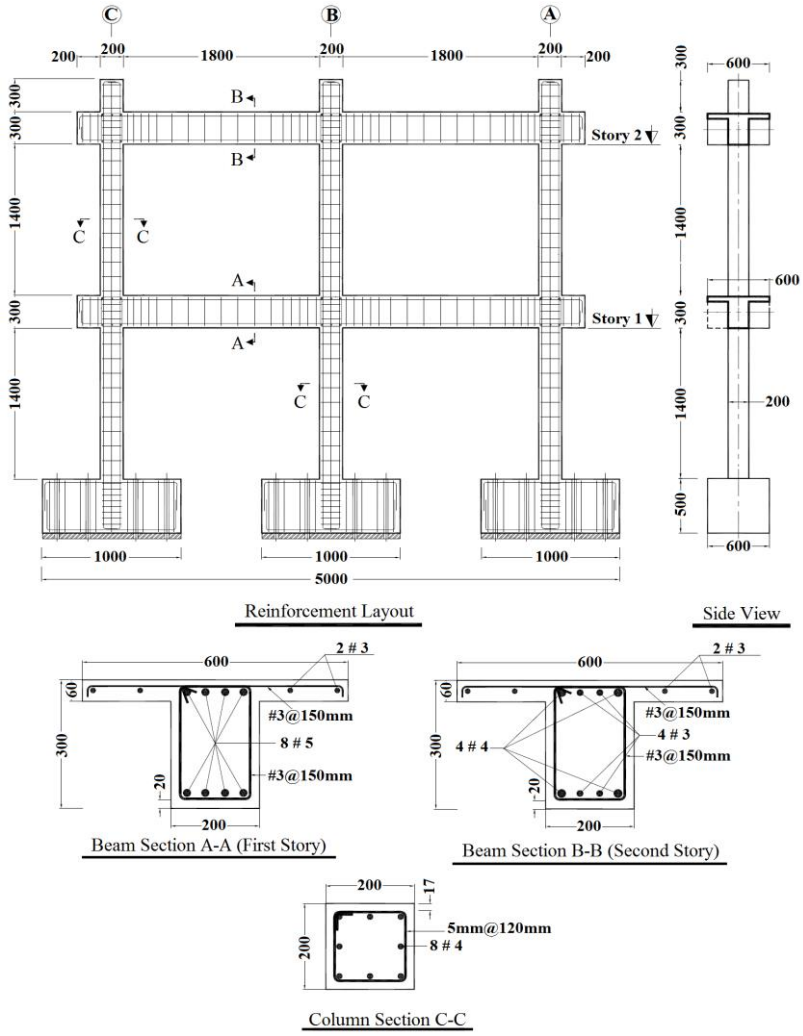

Fig. 1. Schematic scheme of the tested frame MUFS (Yavari et al., 2008) [13].

To calibrate the analytical model with experimental test results, the Limit State material [8] implemented at OpenSees [31] program is considered to model shear and axial failure [30].

To account slip behavior at the end of members, an elastic rotational spring (Eq. 3) using zero-length element [39], is modeled.

$$K_{slip} = \frac{8u}{d_b f_s} EI_{flex}(MPa) \quad (3)$$

Where, u is the bond stress (assumed to be $0.8\sqrt{(f'_c)}$, MPa); d_b is the nominal diameter of the longitudinal reinforcement, f_s is the yield tensile stress in the longitudinal reinforcement, and EI_{flex} is the effective flexural stiffness. The effective flexural stiffness is calculated from moment-

curvature analysis of a column section. Figure 2 shows the scheme of modeling which is used in this paper.

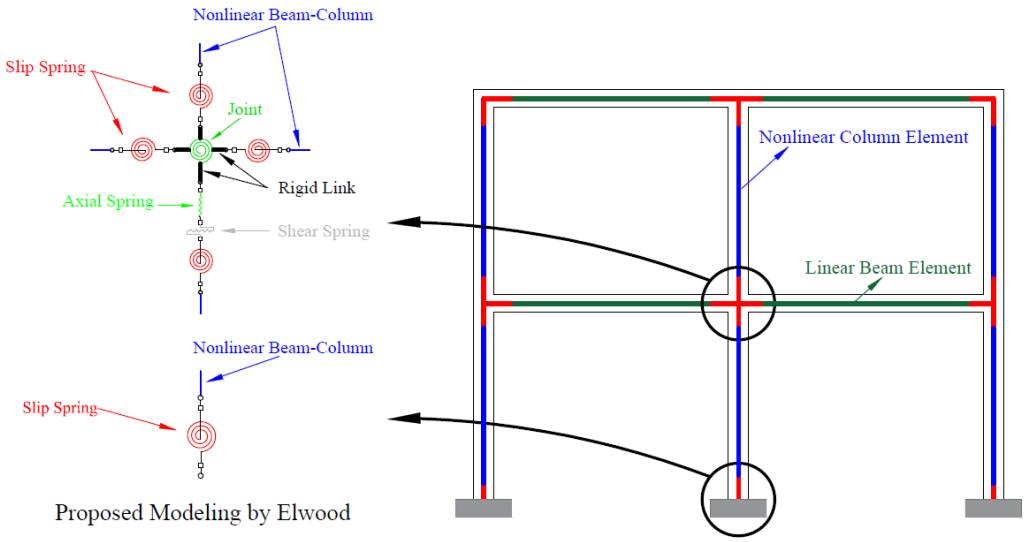

Fig. 2. Schematic presentation of the frame model.

Based on observed damages reported by researchers, the beams and joints remained elastic, and hence, the nonlinear behavior is not assigned here in Fig 2 [13,38]. In the model, five gauss integration points are defined along the columns. The effect of damping was considered in the model using Rayleigh damping, and a damping ratio of 0.02 is assigned to the first two modes of the structures.

The used ground motion in shaking table test was Chi-Chi earthquake (1999 – Station TCU047) with the PGA of 0.40g. Three tests were carried out with the scaled PGA of 0.30g, 1.10g, and 1.35g. The natural period of the frame was measured 0.29 second. The results of nonlinear analysis and experimental results are plotted together in Figure 3. The comparison shows acceptable convergence between the obtained results such as shear failure, maximum drift ratio, and maximum base shear.

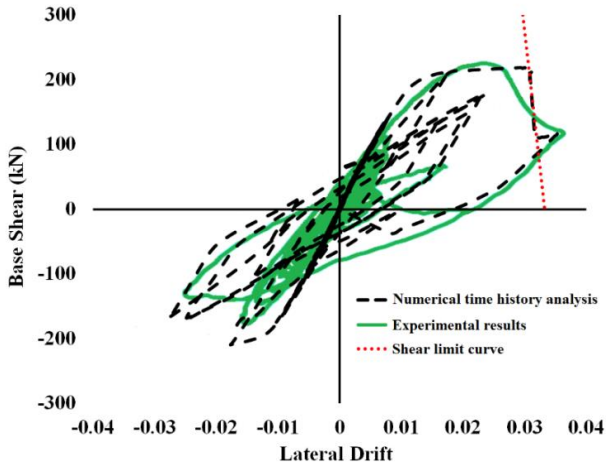

Fig. 3. The comparison of numerical and experimental models via Non-linear time history analysis.

3. Considered Non-ductile reinforced concrete buildings

3.1. General properties of frames

In this paper, two models as representative of old non-ductile R.C in Iran are considered; a frame with 3 stories and 3 bays and another one with 5 stories and 2 bays. The mentioned models are more consistent with existing non-ductile RC buildings in Iran. For analyzing purpose, an interior frame is chosen and analyzed as a 2D frame as shown in Figure 4. The height of columns and the span length for all models are 3200 and 4000 mm respectively. The Young's modulus and the Poisson's ratio for concrete were set to 24000 MPa and 0.2, respectively. For reinforcing steel, The Young's modulus and the Poisson's ratio were set to 200 GPa and 0.3, respectively. The yield stress of longitudinal and transverse reinforcement was selected as 300 MPa, and the compressive strength of concrete was 20 MPa. All geometric and mechanical characteristic values are common for residential and office buildings in Iran. Figure 5 illustrates two different modeling approaches, which are employed in this study, proposed by Elwood (2002) and ASCE/SEI 41. The nonlinear modeling approach, proposed by Elwood, describes the flexure-shear-axial behavior of reinforced concrete columns by means of slip, shear, and axial springs, respectively. More information regarding this nonlinear modeling method can be found in [28,29]. On the other hand, ASCE/SEI 41 proposes criteria for the occurrence of flexure, shear and axial failure based on geometry and mechanical properties of RC columns. Hence, force-rotation relations for concrete columns were assigned to the rotational spring, located at the top of columns, by means of the three-line curve which will be further described in sec. 4.2. In this paper, three models for each approach are considered. These three models can be stated based on the initial axial load ratio of columns and the transverse reinforcement spacing in columns ($P/Ag.f'c$ – S(mm)) as; 0.12–200, 0.17–250 and 0.25–300.

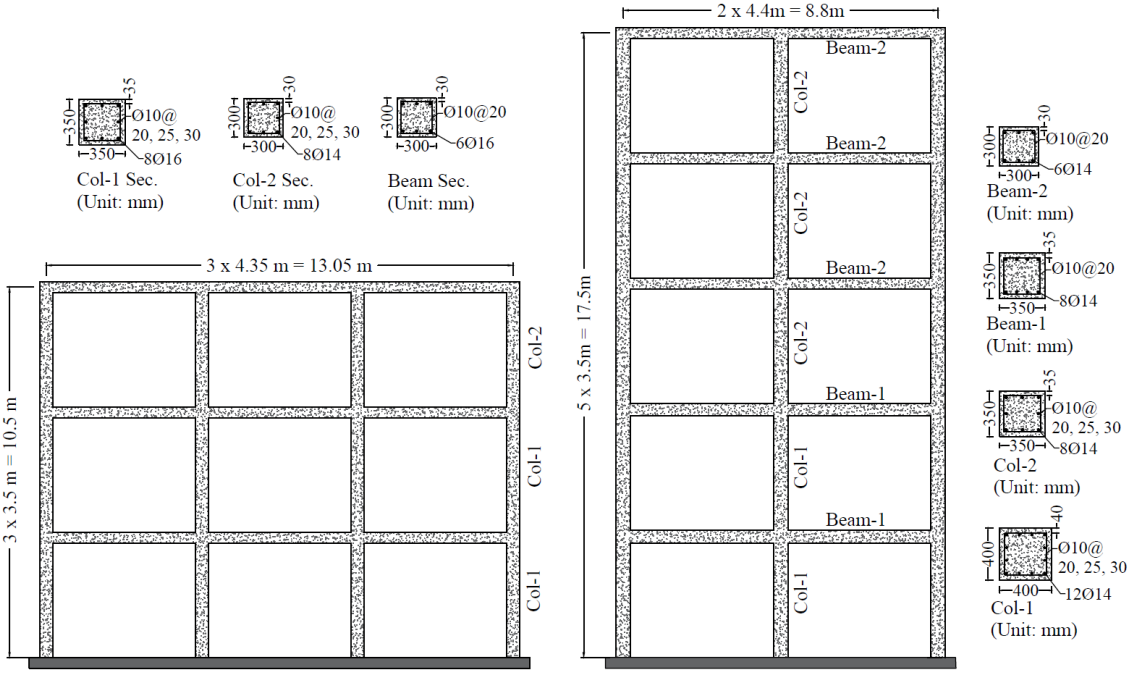

Fig. 4. Elevation view and structural details of case study frames.

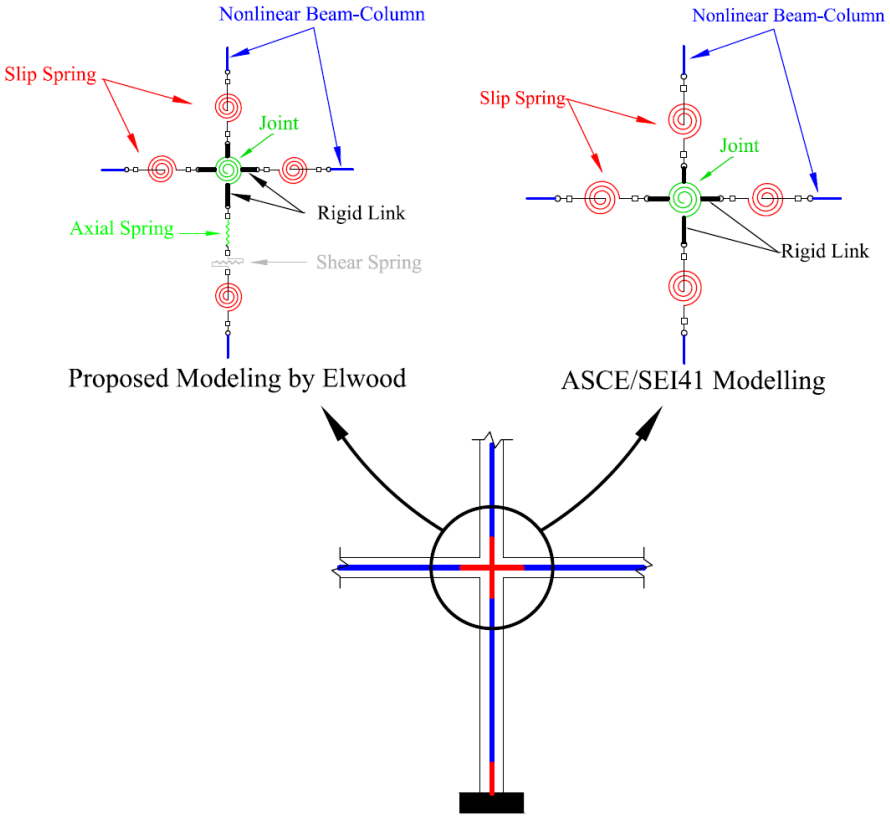

Fig. 5. Schematic presentation of 3 and 5 story models.

It is important to note that, the authors' field survey showed that, all the past old R.C. buildings have not necessarily beams stronger than columns. Representatives models here are selected based on average of those exist in Iran. Therefore, the beam and column elements are modeled using nonlinear beam-column element, which is a structural elements. It is worthwhile to note that using micro-modeling techniques such as continuum elements is another widely employed option, mostly in research objectives, which can provide more detailed investigations; however, it is computationally more expensive than conventional macro-modeling structural elements, but it may provide more detailed information.

Two modeling approaches for flexure-shear-axial interactions are considered; shear-axial spring model, and ASCE-41 global model. The period of 3 and 5-story models was measured 0.96 and 1.31 second respectively. The term of mass was assigned as a concentrated mass to the top of columns. All beams for both modeling techniques were modeled using non-linear fiber section and joints were modeled using rotational spring.

4. Modeling parameters and approaches

4.1. Shear-axial springs model

In this approach, the coupled shear- axial springs were modeled at the top of columns as described in Sec. 3.1. At this empirical-based modeling technique, shear and axial springs are limit state uniaxial materials with shear and axial limit curves respectively. Slip springs were

located at the bottom of columns to consider the effect of strain penetration of longitudinal bars. Nonlinear beam-column elements connect two zero-length elements located at the top and bottom of columns. Beams were modeled using nonlinear beam-column element, and slip springs were located at both ends of beams. To model the behavior of joints, the prescribed parameters of ASCE/SEI41-13 [31] for Non-ductile reinforced concrete joints, were implemented. Figure 6 shows the assigned shear force-rotation curves for the joints with initial axial load ratio of 0.12. The joint behavior curves in other models with the initial axial load ratio of 0.17 and 0.25 follow the same manner.

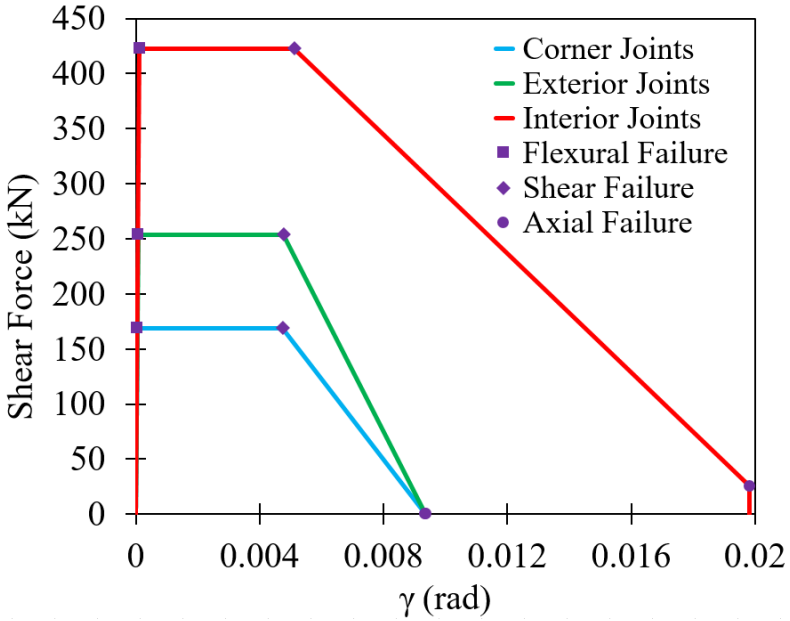

Fig. 6. Shear Force Vs. Rotation of the joints for the model with P/Ag.f'c =0.12 (ASCE/SEI 41).

Fig. 6 demonstrates that the strength and ductility capacities of the modeled joints considerably vary based on the location of joints. This can be described as the effects of confinement on the terms of strength and ductility. On the other hand, it was observed that with increasing the axial load in columns, the ductility capacity decreases.

4.2. ASCE/SEI-41 method

This approach was developed according to ASCE/SEI41-13 [31] concrete provision. In this modeling technique, flexure, shear, and axial springs were removed and a moment-rotation spring defined to consider the flexure-shear-axial behavior in columns. All rest details are the same of the previous modeling technique. Figure 7 shows a sample of defined shear force-rotation curves for the columns in 3 story frame according to the variation of initial axial load ratios. In figure 7, the shear force is estimated by the sum of shear strength carried by concrete and stirrups.

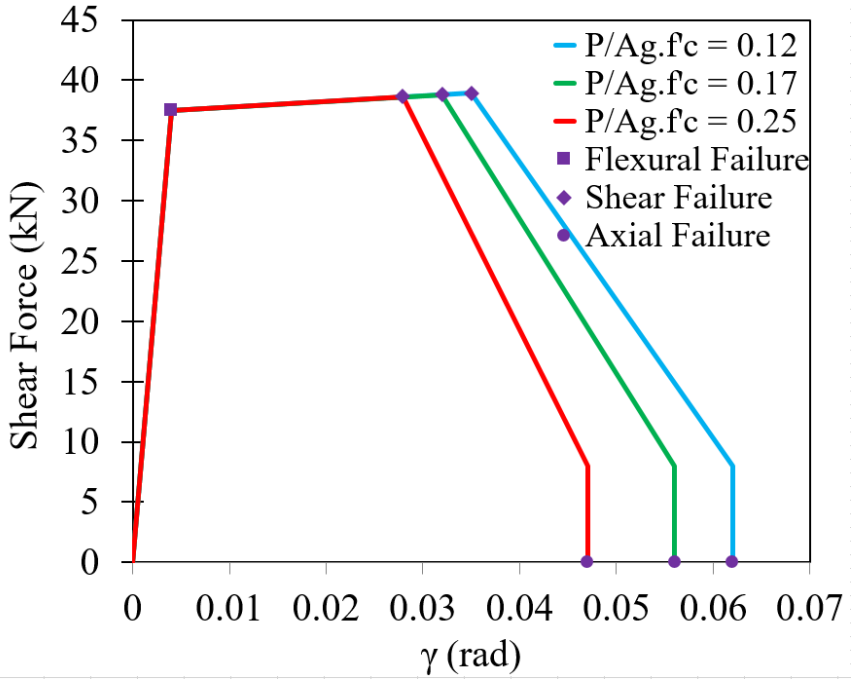

Fig. 7. Shear Force Vs. Rotation curves for the columns in 3 story frame according to the variation of initial axial load ratios (ASCE/SEI 41-13).

Both three and five-story models were categorized using three initial axial load ratios (*P/Ag.f'c* = 0.25, 0.17 and 0.12) and three spacing of transverse reinforcement (*S*= 300, 250 and 200 mm).

5. The Pushover Analysis

The results of the push-over analysis can present the mechanism of collapse initiation in buildings. The obtained results due to pushover analysis for 3 and 5-story models are shown in Figure 8. Figure 8 illustrates the response of base shear versus roof drift ratio regarding three axial load ratios and spacing of transverse reinforcement as well as two mentioned modeling approaches. As expected, decreasing of initial axial load ratio and spacing between stirrups for the models with shear and axial springs cause an increasing of drift ratio at shear and axial failure. All models have the same behavior until the occurrence of the first shear failure. However, when first shear failures were detected, the models experience strength degradation. After the occurrence of the first shear failure, the rate of strength degradation is different. The models with shear-axial spring show sudden strength loss, and consequently, first axial failure terminate the analysis. Unlike this model, modeling based on ASCE-41-13 [31] shows less strength degradation after first shear failure, and displacement ductility increases more than shear-axial spring models. The occurrence of an axial failure in this model can not limit increasing of displacement capacity until a numerical divergence terminates the run. It is important to note that, the first axial failure in this model (ASCE-41 model) just loses the lateral capacity of the same column and the last axial failure (as indicated in Figure 8) does not necessarily happen in the same story. It may occur in another story. Hence, after first axial failure, the shear capacity necessarily has not sudden drop up to shear-axial spring model.

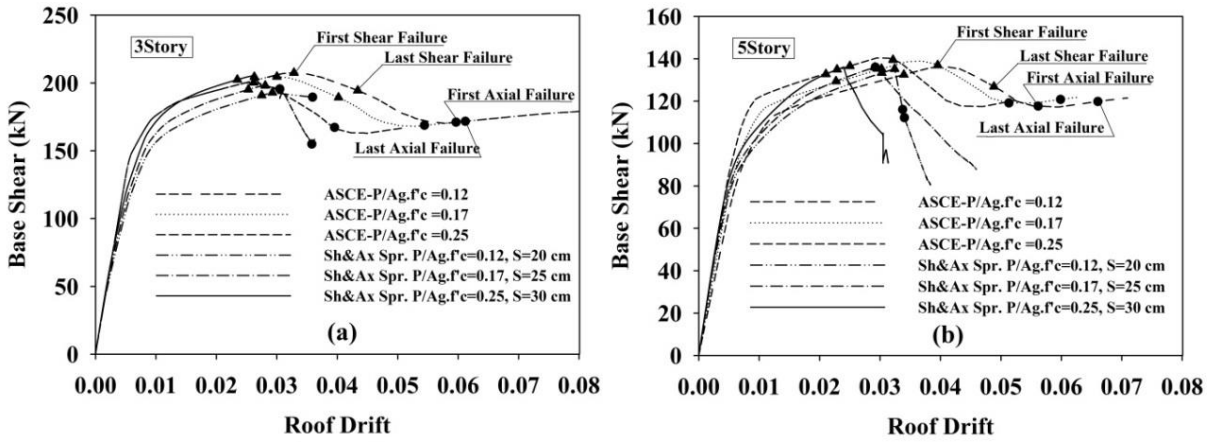

Fig. 8. Base shear - Roof drift plot due to non-linear pushover analysis in (a) 3-Story models and (b) 5-Story models.

The global gravity collapse in non-ductile columns mostly appears after the occurrence of an axial failure. In other words, in a floor when the axial capacity of a single column is lost, the other columns can carry the distributed weight from the first failed column. In this circumstance, the quality of beams performance is crucial. If the beams can bridge between remained columns and no failure appears in the beams, it is expected that the remained columns can carry excessive demanded loads until their ultimate axial capacities are met. To investigate the difference between first and global axial failure, all models have been assessed. Figure 9 shows a sample of results. Figure 9a illustrates the axial load in a column that experience axial failure (first axial failure) versus axial displacement. Figure 8b shows the sum of axial loads in story's columns versus axial displacement. As shown in Figure 9a the initial axial load in column increases (due to overturning actions) until at displacement of 0.25 cm, axial failure is detected. In the same manner, axial load of floor illustrated in Fig. 8b is constant up to first axial failure. Rationally, after first axial failure, the total axial force should be constant, if the lost weight can transmit to other columns. The analysis results show that, due to numerical problems, the program was not able to consider more steps of pushover analysis after detection of an axial failure.

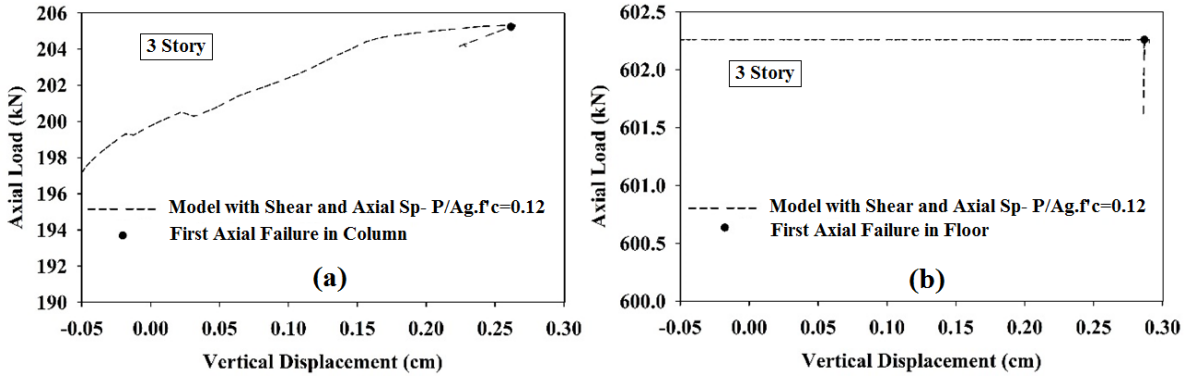

Fig. 9. Axial Load – Vertical Disp. plot due to non-linear pushover analysis in 3-Story model (a) the first axial failure in the column and (b) the first axial failure in the floor.

The numbers of brittle responses in columns at higher drift ratio can produce numerical instability in responses. So in current research, the first axial failure and global gravity failure are assumed the same, and in the remaining discussion, no difference is made between them.

6. Earthquake records properties

To perform time history analyses in OpenSees due to far-field records, twelve records were chosen from FEMA P695 [39]. The magnitude of records varies between 6.5-7.5, the site distance is between 7.1-23.6 km, and the peak ground accelerations are between 0.21g-0.53g.

The graphs of pseudo-Acceleration versus period for the mentioned records are shown in figure 10.

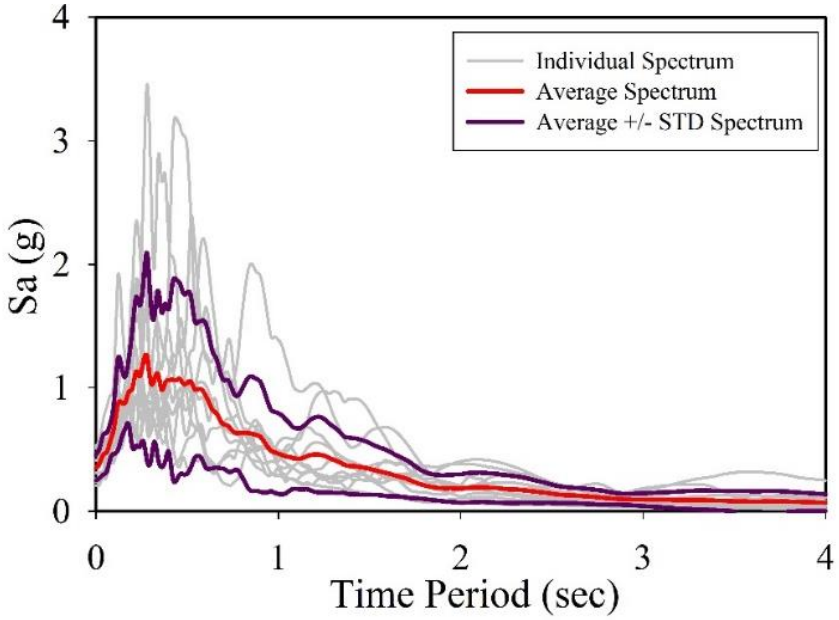

Fig. 10. The Sa(g) of applied records vs. time period.

7. Incremental dynamic analysis of modeled buildings

Incremental dynamic analysis (IDA) is a collection of non-linear dynamic analyses that uses several spectra accelerations. Scaled intensity measure (IM) is chosen to consider linear and non-linear situations of a structure and eventually lateral dynamic instability.

In this study, twelve models are considered to conduct IDA (two buildings, two modeling approaches, three axial load ratios and transverse reinforcement spacing). Each model is analyzed under twelve far-filed records to determine the shear and axial failure in columns. To this end, at first, the IDA curves are developed for every twelve models. The IDA curves show the spectra acceleration at fundamental period of buildings versus maximum inter-story drift. The Figures11 and 12 show the sample of results of IDA curves for three and five-story building models respectively with the same axial load ratio and transverse reinforcement spacing. In the plotted curves in Figures 11 and 12, the black triangles and circles show the point of first shear

and axial failure respectively, and black stars indicate the point of lateral dynamic instability. The dynamic instability point has defined the point on curves that, with a small increase in lateral acceleration, infinite inter-story drift ratio can achieve. The two points should be paid attention. The first point is that many of IDA curves have not attained dynamic instability due to numerical divergence encountered after axial failure and hence, dynamic instability is not addressed in curves. The second point is that in some cases, the indicated point as dynamic instability is before axial failure point which is turned to our judgment on indicating a point as dynamic instability. This matter can not affect our purposes from this research. As a result of Figures 11 and 12, following few steps of analysis after first axial failure, the model becomes unstable and analysis is terminated. Therefore, in current research, the point of occurrence of first axial failure can be considered as instability state.

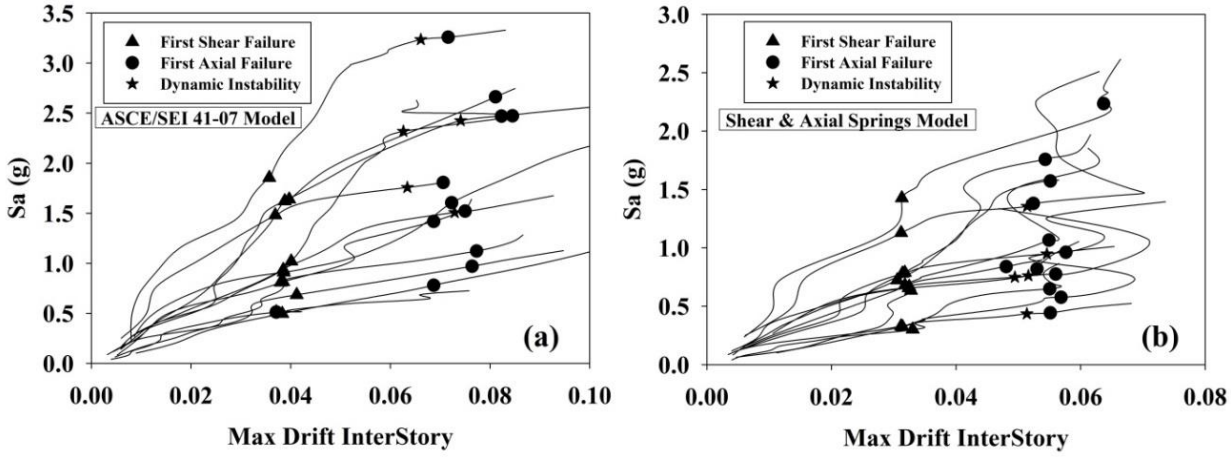

Fig. 11. Sa (g) Vs. Maximum Inter-story drift ratio for 3-Story model with P/Ag.f'c =0.12, S=200 mm. a) ASCE/SEI 41-13 modeling approach, b) shear and axial springs modeling approach.

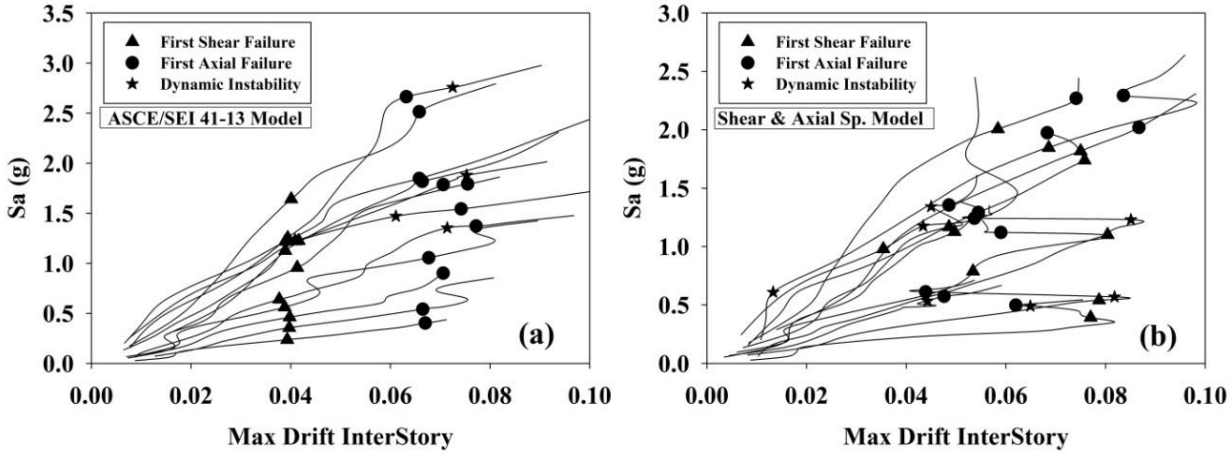

Fig.12. Sa (g) Vs. Maximum Inter-story drift ratio for 5-Story model with P/Ag.f'c =0.12, S=200mm. a) ASCE/SEI 41-13 modeling approach, b) shear and axial springs modeling approach.

The derived results from Figures 11 and 12 are shown in Table 3. Moreover, for comparison, the results of pushover analysis on both modeling techniques are also listed in Table 1.

Table 1
The mean of maximum inter-story drift ratio at first shear and axial failure derived from IDA.

No. of Story	Modelling approach	Type of Failure	$P/A_g.f'_c = 0.12$ S=200 mm		$P/A_g.f'_c = 0.17$ S=250 mm		$P/A_g.f'_c = 0.25$ S=300 mm	
			Time History (%)	Push over (%)	Time History (%)	Push over (%)	Time History (%)	Push over (%)
3 Story	Elwood	Shear	3.19	2.75	3.07	2.53	2.86	2.35
		Axial	5.59	3.59	4.67	3.05	2.86	2.35
	ASCE	Shear	3.85	3.28	3.51	3.00	3.08	2.62
		Axial	7.66	5.97	6.64	5.44	3.08	2.62
5 Story	Elwood	Shear	5.79	3.24	4.39	2.27	3.59	2.10
		Axial	6.52	3.37	5.35	2.92	3.59	2.10
	ASCE	Shear	3.97	3.39	3.55	3.02	3.28	2.50
		Axial	7.15	5.62	6.18	5.13	3.28	2.50

The results of Table 1 demonstrate that both modeling approaches in two considered frames nearly present the same shear and axial drift ratios, except that the modeling based on shear-axial springs, the values of drift ratio at first shear failure of five-story buildings are more than 3-story frame as 25%-81%. The mentioned differences become smaller where axial load ratio increases from 0.12 to 0.25. At all listed results in Table 3 with increasing axial load ratio from 0.12 to 0.25 the reported values on both modeling approaches and frames show the fewer differences and smaller values of drift ratio. For instance, for an axial load ratio of 0.25, all resulted values are nearly resembled, and less dispersion can be seen in results. The results also reveal that with increasing in axial load ratio, the difference between first shear failure and first axial failure become negligible. In comparison between two modeling approaches, the following results can be inferred:

- In 3-story frame for all axial load ratio, the drift ratio at first shear failure from modeling with shear-axial springs is less than that of ASCE-41-13 approach as 7%-17%, while in the 5-story frame, it is inverse (45%-10%).

- Both frames and both modeling approaches have shown that the values of drift ratio at first axial failure from shear-axial springs model are less than ASCE-41/13 approach. The differences vary between 7%-17% for the 3-story frame and 9%-14% for the 5-story frame. An exception is for the 5-story frame at axial load ratio 0.25 which can be assigned to the dispersion of IDA results.

The results listed in table 3 show that push-over analysis almost underestimates the first shear and axial failure in comparison with IDA particularly at the 5-story frame and for lower axial load ratio.

In section 4, the probability of global collapse occurrence after axial failure in a floor due to non-linear pushover analysis investigated. In this section, the occurrence of global collapse is investigated in all models with shear and axial springs. A sample result of models with initial axial ratios of 0.12 in the 3-Story model due to non-linear time history analysis is shown in Figure 13.

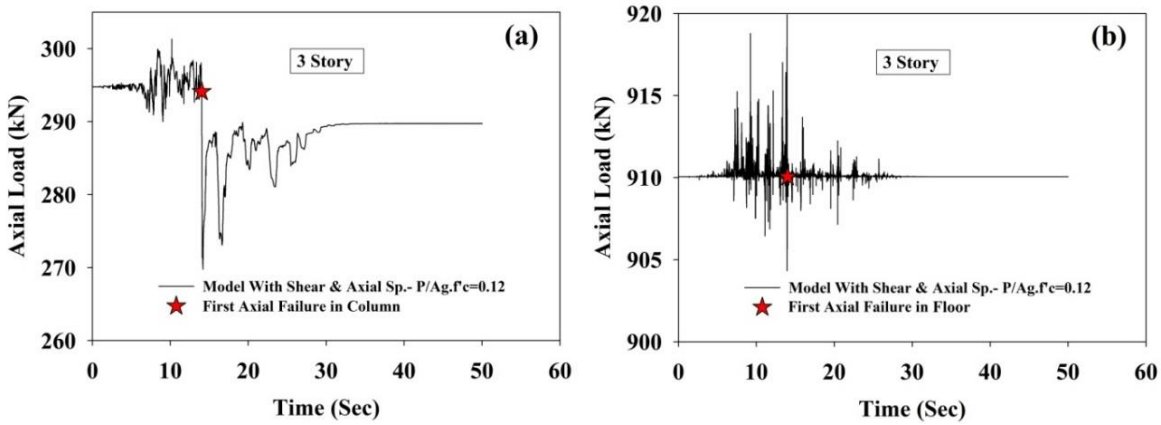

Fig. 13. Axial load versus time in 3-Story model, (a) in a column suffered axial failure, (b) in the floor including the column which suffered axial failure.

In Figure 13, the graph of axial load versus time for a column and floor is presented. In Figure 13, the column and floor experienced the first axial failure due to non-linear time history analysis. According to Figure 13a, the axial load capacity of column decrease around 10% after axial failure initiation, whereas the axial load capacity of floor did not change significantly (Figure 13b). The results of the assessment on other columns show that losing axial load at failed column due to axial failure redistribute on other columns. However, the sum of axial load capacity of columns in a floor did not change significantly. However as stated in section 4, due to convergence problems no much more drift is seen after first axial failure. The same conclusion discussed in section 4, is inferable here and for brevity not explained again. Therefore, no significant differences can consider between first axial failure and global axial failure in low-rise buildings.

8. Seismic fragility assessment

The conditional seismic demand in reinforced concrete columns for each record and each spectral acceleration may be calculated using lognormal distribution as follows:

$$P = 1 - \Phi\left(\frac{\ln(S_a * g) - \lambda}{\xi}\right) \tag{4}$$

Where, Φ is a logical value that determines the form of function, *Sa* is pseudo acceleration, g is gravity acceleration, λ is mean deviation and ξ is a standard deviation for each pseudo acceleration in shear and axial failure. So, the fragility curve is calculated using the following equation:

$$FR = \Phi\left(\frac{\ln((S_a * g) / \lambda)}{\xi}\right) \quad (5)$$

The results of statistic calculations for all analyzed models are presented in Table 2, where λ and ξ are mean and standard deviation of spectral accelerations respectively.

Table 2
Statistic results of the calculation of mean and standard deviation.

Number of Story	Modelling Approach	Type of Failure	$P/A_g.f'_c = 0.25$ S=300 mm		$P/A_g.f'_c = 0.17$ S=250 mm		$P/A_g.f'_c = 0.12$ S=200 mm	
			λ	ξ	λ	ξ	λ	ξ
3 Story	Elwood	Shear	1.728	0.493	1.751	0.494	1.836	0.491
		Axial	1.728	0.493	2.051	0.429	2.262	0.482
	ASCE	Shear	2.002	0.449	2.167	0.443	2.256	0.446
		Axial	2.002	0.449	2.653	0.503	2.795	0.453
5 Story	Elwood	Shear	1.712	0.564	1.969	0.573	2.037	0.557
		Axial	1.712	0.564	2.169	0.559	2.478	0.534
	ASCE	Shear	1.797	0.584	1.954	0.597	2.043	0.605
		Axial	1.797	0.584	2.524	0.628	2.573	0.586

The results of Table 2 show that the statistic parameters for shear and axial failure in all models with initial axial load ratio of 0.25 and the spacing of transverse reinforcement of 300 mm, are the same. The main reason refers to Eq. 1 and 2 which axial failure occurs simultaneously with the onset of shear failure. The other models follow failure mode of flexure-shear-axial respectively.

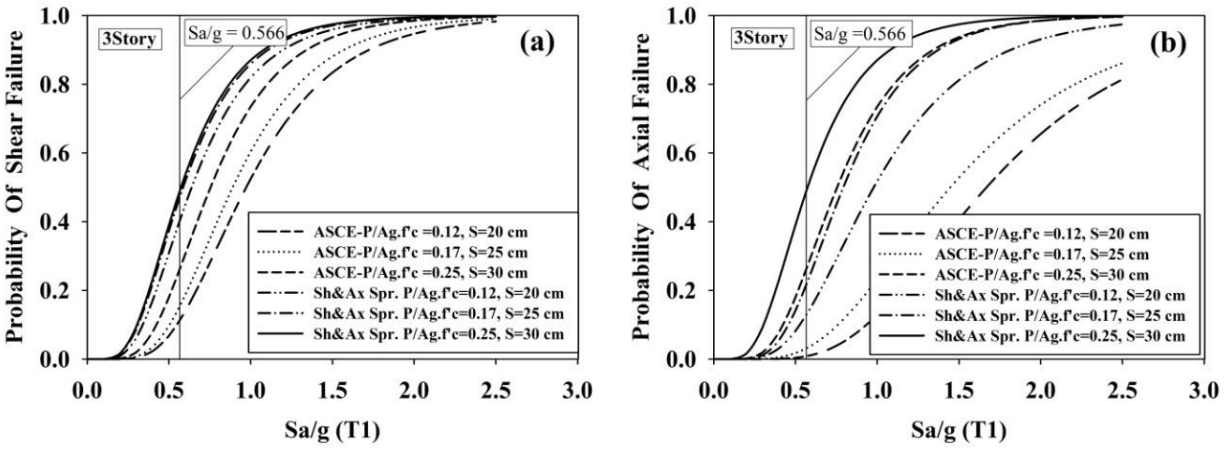

Fig. 14. Seismic fragility curves of shear and axial failure for the 3-story models, (a) probability of first shear failure, (b) probability of first axial failure.

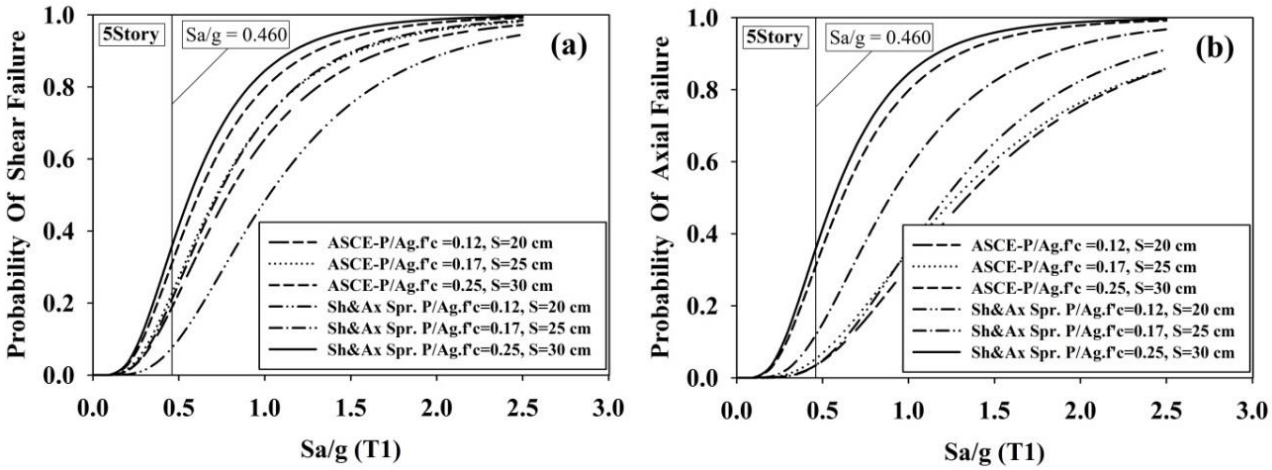

Fig. 15. Seismic fragility curve of shear and axial failure for 5-story models, (a) probability first shear failure, (b) probability first axial failure.

The fragility curves for all models are illustrated in Figures 14 to 15. In Figure 14 and 15, the probability of shear failure (PoS) and axial failure (PoA) for 3 and 5-story frames in companion with two modelling approach, and different axial load ratios and transverse reinforcement spacing, are compared.

To investigate seismic fragility assessment, the values of spectral acceleration at first natural period of each frame are illustrated in both Figures 14 and 15 by a vertical solid line and relevant values. As seen from both Figure 14 and 15, generally the fragility curves at axial failure are wider than shear failure curves. As a general concluding, the probability of failure attained by shear-axial spring modeling approach, are more than ASCE-41 modeling approach. To compare the value of failure probability, Table 3 is presented. In Table 3 the values of probability of failure for all models are listed.

Table 3
The Probability of shear and axial failure at first natural period of each frame for two employed modeling approach.

No. of Story	Type of Failure	$P/A_g.f'_c = 0.25$ S=300 mm			P/Ag.f'c = 0.17 S=250 mm			P/Ag.f'c = 0.12 S=200 mm		
		Prob. of Failure (%)			Prob. of Failure (%)			Prob. of Failure (%)		
		Elwood	ASCE	Diff. (%)	Elwood	ASCE	Diff. (%)	Elwood	ASCE	Diff. (%)
3 St.	Shear	48.8	26.0	87	47.8	**15.5**	209	40	**11.3**	255
	Axial	48.8	26.0	87	21.9	**3.4**	539	**13**	**3.0**	330
5 St.	Shear	35.7	31.1	14.	21.1	22.7	7	**7.9**	18.8	58
	Axial	35.7	31.1	14.	**12.3**	**5.2**	137	**3.6**	**3.4**	4

Table 3 reveals that in most cases, the PoS and PoF derived from modeling based on shear-axial spring are more than ASCE-41 approach. An exception is PoS in 5-story frame for axial load

ratio 0.12 which can be due to dispersion in results. The differences between PoS and PoF due to two modeling approaches are also listed in Table 3. The listed values show that the differences between the obtained results for two modeling techniques do not follow a clear procedure, however with increasing in axial load ratio from 0.12 to 0.25, dispersion becomes smaller.

8.1. Comparison with the level of safety probability of failure suggested by ASCE-41

ASCE-41-13 considers the level of safety when proposed modeling parameters for nonlinear analysis. The goal in selecting values for modeling parameters in non-ductile concrete columns is to achieve a high level of safety probability of failure less than 15% for columns that may experience shear failures, while allowing a slightly lower level of safety 35%, for columns expected to experience flexural failures. Given the potential of collapse resulting from axial load failure of individual columns, a high level of safety 15% is desired. It emphasizes that the target limits for probabilities of failure were selected based on the judgment of Ad Hoc Committee. To investigate the reliability of proposed modeling parameters and compare the results of two modeling approaches on buildings responses, in Table 5 those PoS or PoF less than 15% are bolded. The numbers of bolded items show that many cases do not meet such target. Except for frames with lower axial load ratio, it can be concluded that no other cases can pass the mentioned target. Although the proposed rotation values in ASCE-41 on shear and axial failure of columns have resulted from experimental tests and proposed target values, have considered columns test and judgment as a whole. However, it seems the probability of failure on the building should be considered where the modeling parameters are suggested.

9. Summary and conclusion

In this paper, the main purpose was to investigate the prediction of the drift ratio capacity at shear and axial failure in existing RC columns in framed buildings due to the earthquake. Therefore, six numerical models were developed according to two modeling techniques, as the models with shear and axial springs at the top of columns and the models based on ASCE/SEI 41-13 concrete provisions. The results of push-over analysis and IDA were processed and using fragility curves the following conclusions are inferred:

- No meaningful difference in drift ratios between first axial failure, story gravity failure, and lateral instability was achieved. Almost all cases became unstable after first axial failure detection.
- In comparisons between two modeling approaches, the method of ASCE-41-13 over-estimates first axial failure than modeling with shear-axial springs. In shear failure detection, the specific conclusion was not achieved.
- The derived results showed that pushover analysis underestimates drift values at shear and axial failure in comparison with IDA results.
- The results of fragility curves showed that the probability of failure attained by shear-axial spring modeling approach, are more than ASCE-41 modeling. The differences between results of two modeling techniques do not follow a clear procedure; however, with

increasing in axial load ratio from 0.12 to 0.25 and transverse reinforcement spacing from 200-300 mm, dispersion becomes smaller.

- the results of probability of failure for shear and axial failure corresponding to spectral acceleration at first natural period (Sa(T1)) showed that, where axial load ratio or spacing of transverse reinforcements become larger (from 0.12-0.25 for both modelling approaches), the level of safety cannot pass the level of safety target suggested by ASCE-41-13(i.e. 15% probability of shear and axial failure on columns).

References

[1] Allahvirdizadeh R, Mohammadi MA. Upgrading equivalent static method of seismic designs to performance-based procedure. Earthquakes Struct 2016;10:849–65. doi:10.12989/eas.2016.10.4.849.

[2] Allahvirdizadeh R, Khanmohammadi M, Marefat MS. Probabilistic comparative investigation on introduced performance-based seismic design and assessment criteria. Eng Struct 2017;151:206–20. doi:10.1016/j.engstruct.2017.08.029.

[3] Shafaei S, Ayazi A, Farahbod F. The effect of concrete panel thickness upon composite steel plate shear walls. J Constr Steel Res 2016;117:81–90. doi:10.1016/j.jcsr.2015.10.006.

[4] Rassouli B, Shafaei S, Ayazi A, Farahbod F. Experimental and numerical study on steel-concrete composite shear wall using light-weight concrete. J Constr Steel Res 2016;126:117–28. doi:10.1016/j.jcsr.2016.07.016.

[5] Ayazi A, Ahmadi H, Shafaei S. The effects of bolt spacing on composite shear wall behavior. World Acad Sci Eng Technol 2012;6:10–27.

[6] Shafaei S, Farahbod F, Ayazi A. Concrete Stiffened Steel Plate Shear Walls With an Unstiffened Opening. Structures 2017;12:40–53. doi:10.1016/j.istruc.2017.07.004.

[7] Shafaei S, Farahbod F, Ayazi A. The wall-frame and the steel-concrete interactions in composite shear walls. Struct Des Tall Spec Build 2018:e1476. doi:10.1002/tal.1476.

[8] Elwood KJ. Shake table tests and analytical studies on the gravity load collapse of reinforced concrete frames. 2004.

[9] Elwood KJ, Moehle JP. Evaluation of existing reinforced concrete columns. Proceedings, 2004.

[10] Elwood KJ. Modelling failures in existing reinforced concrete columns. Can J Civ Eng 2004;31:846–59. doi:10.1139/l04-040.

[11] Elwood KJ, Moehle JP. Dynamic Shear and Axial-Load Failure of Reinforced Concrete Columns. J Struct Eng 2008;134:1189–98. doi:10.1061/(ASCE)0733-9445(2008)134:7(1189).

[12] Kabeyasawa T, Kabeyasawa T, Kim Y. Progressive Collapse Simulation of Reinforced Concrete Buildings Using Column Models with Strength Deterioration after Yielding. Improv. Seism. Perform. Exist. Build. Other Struct., Reston, VA: American Society of Civil Engineers; 2009, p. 512–23. doi:10.1061/41084(364)47.

[13] Yavari S, Lin SH, Elwood KJ, Wu CL, Hwang SJ, Moehle JP. Study on collapse of flexure-shear-critical reinforced concrete frames. 14th World Conf. Earthq. Eng. Beijing, China, 2008.

[14] Yavari S, Elwood KJ, Wu C. Collapse of a nonductile concrete frame: Evaluation of analytical models. Earthq Eng Struct Dyn 2009;38:225–41. doi:10.1002/eqe.855.

[15] Mosalam KM, Talaat M, Park S. Modeling progressive collapse in reinforced concrete framed structures. Proc. 14th World Conf. Earthq. Eng., 2008, p. 12–7.

[16] Wu C, Kuo W-W, Yang Y-S, Hwang S-J, Elwood KJ, Loh C-H, et al. Collapse of a nonductile concrete frame: Shaking table tests. Earthq Eng Struct Dyn 2009;38:205–24. doi:10.1002/eqe.853.

[17] Matamoros AB, Matchulat L, Woods C. Axial load failure of shear critical columns subjected to high levels of axial load. Proc. 14th World Conf. Earthq. Eng, Citeseer; 2008.

[18] Nakamura T, Yoshimura M. Gravity Load Collapse of Reinforced Concrete Columns with Brittle Failure Modes. J Asian Archit Build Eng 2002;1:21–7. doi:10.3130/jaabe.1.21.

[19] Nakamura T, Yoshimura M. Simulation of Old Reinforced Concrete Column Collapse by Pseudo-dynamic Test Method. World Conf. Earthq. Eng., vol. 12, 2012, p. 1–10.

[20] Mostafaei H, Vecchio FJ, Kabeyasawa T. Nonlinear displacement-based response prediction of reinforced concrete columns. Eng Struct 2008;30:2436–47. doi:10.1016/j.engstruct.2008.01.020.

[21] Mostafaei H, Vecchio FJ. Uniaxial shear-flexure model for reinforced concrete elements. J Struct Eng 2008;134:1538–47.

[22] Mostafaei H, Vecchio FJ, Kabeyasawa T. Deformation capacity of reinforced concrete columns. ACI Struct J 2009;106:187.

[23] Murray JA, Sasani M. Evaluating System-Level Collapse Resistance of Non-Ductile RC Frames Structures. Proc. 10th Natl. Conf. Earthq. Eng. Earthq. Eng. Res. Institute, Anchorage, AK, 2014.

[24] Henkhaus KW. Axial failure of vulnerable reinforced concrete columns damaged by shear reversals 2010.

[25] Sasani M. Shear Strength and Deformation Capacity Models for RC Columns. 13th World Conf. Earthq. Eng. Vancouver Canada, Pap., 2004.

[26] Kyriakides N, Sohaib A, Pilakoutas K, Neocleous K, Chrysostomou C, Tantele E, et al. Evaluation of Seismic Demand for Substandard Reinforced Concrete Structures. Open Constr Build Technol J 2018;12:9–33. doi:10.2174/1874836801812010009.

[27] Allahvirdizadeh R, Gholipour Y. Reliability evaluation of predicted structural performances using nonlinear static analysis. Bull Earthq Eng 2017;15:2129–48. doi:10.1007/s10518-016-0062-x.

[28] Kakavand MRA. Limit State Material Manual 2007.

[29] McKenna F, Fenves GL, Scott MH. Open system for earthquake engineering simulation. Univ California, Berkeley, CA 2000.

[30] Elwood KJ, Matamoros AB, Wallace JW, Lehman DE, Heintz JA, Mitchell AD, et al. Update to ASCE/SEI 41 Concrete Provisions. Earthq Spectra 2007;23:493–523. doi:10.1193/1.2757714.

[31] ASCE 41-13. Publ Anticip Seism Eval Upgrad Exist Build 2013;Reston, Vi.

[32] Kyriakides NC, Pantazopoulou SJ. Collapse Fragility Curves for RC Buildings Exhibiting Brittle Failure Modes. J Struct Eng 2018;144:04017207. doi:10.1061/(ASCE)ST.1943-541X.0001920.

[33] Kyriakides N, Ahmad S, Pilakoutas K, Neocleous K, Chrysostomou C. A probabilistic analytical seismic vulnerability assessment framework for substandard structures in developing countries. Earthq Struct 2014;6:665–87.

[34] Ahmad S, Kyriakides N, Pilakoutas K, Neocleous K, Zaman Q uz. Seismic fragility assessment of existing sub-standard low strength reinforced concrete structures. Earthq Eng Eng Vib 2015;14:439–52. doi:10.1007/s11803-015-0035-0.

[35] Galanis PH, Moehle JP. Development of collapse indicators for older-type reinforced concrete buildings. Proc. 15th World Conf. Earthq. Eng., 2012.

[36] Baradaran Shoraka M, Yang TY, Elwood KJ. Seismic loss estimation of non-ductile reinforced concrete buildings. Earthq Eng Struct Dyn 2013;42:297–310. doi:10.1002/eqe.2213.

[37] Farahmand H, Reza Azadi Kakavand M, Tavousi Tafreshi S, Hafiz P. The Effect of Mechanical and Geometric Parameters on the Shear and Axial Failures of Columns in Reinforced Concrete Frames. Ciência e Nat 2015;37.

[38] Yavari S, Elwood KJ, Wu CL, Lin SH, Hwang SJ, Moehle JP. Shaking table tests on reinforced concrete frames without seismic detailing. ACI Struct J 2013;110:1001.

[39] (FEMA) FEMA. Quantification of Building Seismic Performance Factors 2009.